Extended Hückel Calculations on the Oxidative Addition Reaction of $(TBA)_2$ $Pt(CN)_4$ with Halogen

Jaejung Ko*, Kuk-Tae Park

Department of Chemical Education, Korea National University of Education, Chungbuk 363-791

Ikchoon Lee, and Bon-Su Lee

Department of Chemistry, Inha University, Incheon 402-751. *Received July 11, 1989*

The mechanism on the oxidative addition reaction of $(TBA)_2$ $Pt(CN)_4$ with Cl_2 has been studied by means of extended Hückel calculations. Among two possible mechanisms, computational calculations demonstrated that the linear approach of Cl_2 to a $Pt(CN)_4$ moiety is more favourable than three-centered transition state. From our calculations, the most stable process is that a $Pt(CN)_4$ moiety interacts with Cl_2 in the linear transition state and the cleavage of Cl-Cl bond in a coordinated halogen occurred spontaneously, giving rise to a trans product by back-attacking a $Pt(CN)_4Cl$ moiety by Cl. The process consists of the comparison in the stability of each intermediate with use of bonding and potential energy.

Introduction

Oxidative addition reaction is of remarkable importance, since nearly all catalytic and many useful stoichiometric process involve oxidative addition reaction.[1] Reactions in which a group, A-B, adds to, and oxidizes, a metal complex, *M* are described as oxidative addition reactions. Although oxidative addition reactions are known for all even d^n configurations, these reactions are better studied for the d^8 and d^{10} compounds.[2] Particularly, the oxidative addition reactions of d^8 transition metal complexes have produced a number of new compounds.[3] Even though many new compounds have been prepared for the d^8 transition metal complexes via oxidative addition reaction, mechanistic studied have little reported.

Recently, Rund and coworker[4] reported the oxidative addition reaction of halogen and pseudohalogen to $(TBA)_2$ Pt $(CN)_4$, leading to trans $(TAB)_2$ $Pt(CN)_4(X)$ (Y) products. They suggested that the oxidative addition reaction presumably proceed with linear transition state(a) as shown below. When the halogen is reacted to d^8 complexes via oxidative

a b

addition reaction, two halide atoms have one of two orientations, either trans or cis depending on the transition metal compound, the addendum and the experimental condition. For such a system, the linear(a) and three-centered transition state(b) have been suggested.[6]

Viewed from two transition state, it is our impetus to check that Rund's suggest is a right one for the mechanism of oxidative addition reaction. Accordingly, we chose the system because we are interested in mechanistic studies on the oxidative addition reaction and little theoretical work has been brought to bear on this subject. As likely mechanisms for the oxidative addition reaction of Cl_2 to a $Pt(CN)_4^{2-}$ moiety, three mechanisms can be proposed as shown below (1a-c). Therefore, computational calculations on each intermediate will help clarify the mechanism of the type 1a-c.

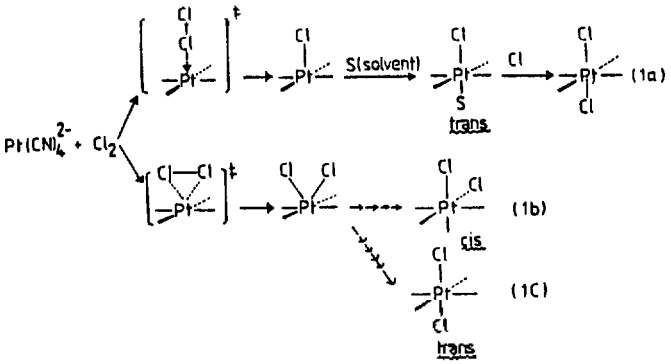

All calculations are of the extended Hückel type[6], and the parameters used are discussed in Appendix.

Linear Transition State. For mechanistic studies on the oxidative addition reaction of $(TBA)_2$ $Pt(CN)_4$ with Cl_2, three mechanisms can be proposed as illustrated in the introduction section. In order to compare the stability and electronic consideration of each intermediate, computational calculations were carried out on each instance. Among three mechanisms, we first deal with the linear transition state.

Figure 1 shows the potential curve for the change of distance between Cl and Pt. Until the distance is over 4 Å, it seems that there is no substantial interaction between two atoms. When the chlorine molecule approaches to the platinum within 3.0 Å in a linear fashion, the interaction is rapidly developed. If the distance is approached in bonding distance, the intermediate would be very unstable. The major contribution for that will be discussed later.

Figure 2 shows the interaction diagram for a chlorine ligand and a $Pt(CN)_4^{2-}$ fragment at the transition state in which the distance between Cl and Pt is 2.34 Å. At the right of the Figure 2 are symmetry adapted linear combinations of the lone pair hybrid on chloride atom. On the left side of the Figure are the metal *s*, *p*, and *d* levels. There is a lower set of two levels, $1b_{2g} + 1a_{1g}$, discended from the 4*d* orbital. At low energy are two filled levels, $2b_{2g} + 1e_g$. At high energy are a filled z^2 character and an empty level primarily of a char-

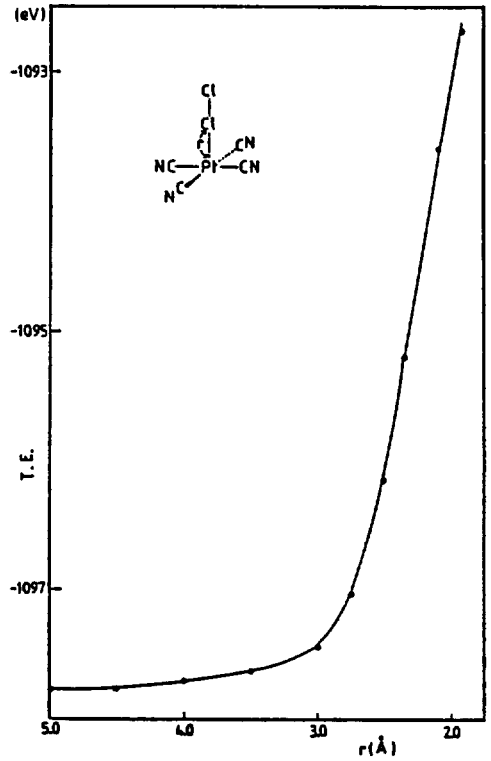

Figure 1. Potential curve for the distance between Cl atom and pt atom.

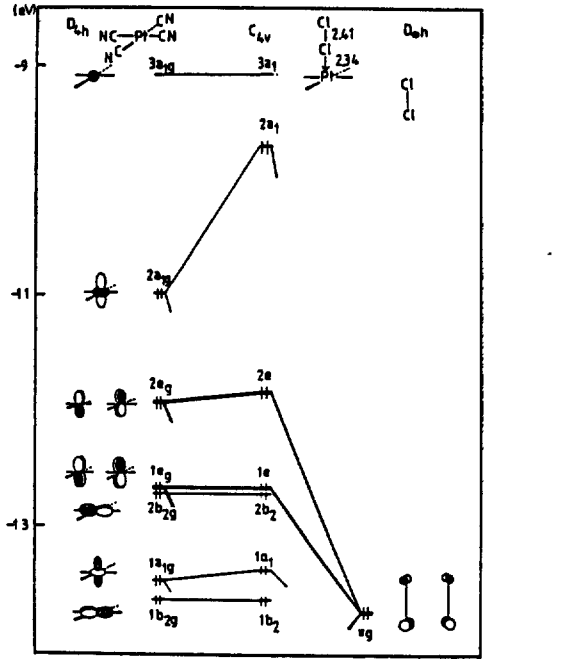

Figure 2. Correlation diagram of orbitals of $Pt(CN)_4Cl_2$ with D_{4h} $Pt(CN)_4$ and $D_{\infty h}$ Cl_2.

acter. At the transition state geometry (middle side of Figure 2), x^2-y^2 and xy remain nonbonding. At middle energy the x and y mix with xz and yz in a bonding and antibonding fashion to produce a Pt-Cl π and π^* bonds, respectively. At higher energy the molecular level, $2a_1$, is made of a combination of z^2 of platinum and $s + z$ of chlorine in an antibonding fashion produce a Pt-Cl σ^* bond. The LUMO, $3a_1$, actually remains nonbonding. The energy gap between HOMO and LUMO is

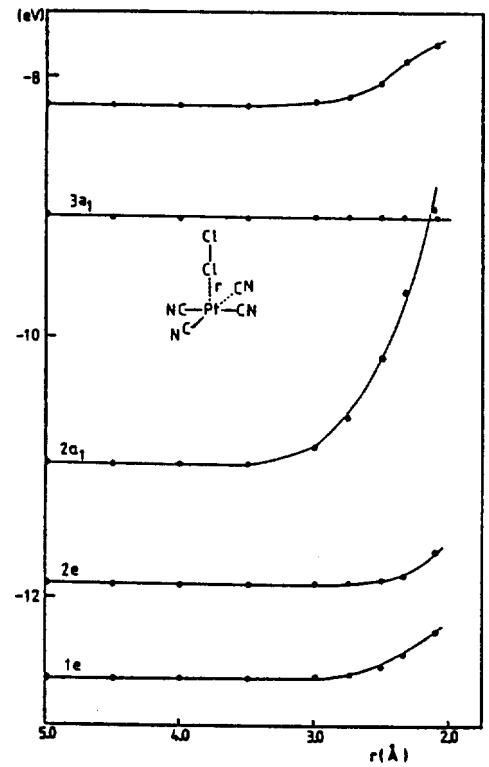

Figure 3. Energy levels of a C_{4v} $Pt(CN)_4Cl_2$ fragment as a function of r.

0.625 eV. Therefore, when the distance between platinum and chlorine is 2.34 Å, there is no problem in the magnetic susceptibility. The unstability of this intermediate arises from a molecular level, $2a_1$, assigned as the HOMO.

Figure 3 shows energy levels of each orbital as a function of r in the intermediate of $Pt(CN)_4Cl_2$. As the distance between platinum and chlorine is shorter, two orbitals, $2e$ and $2a_1$, affect the destabilization of an intermediate. As the mag-

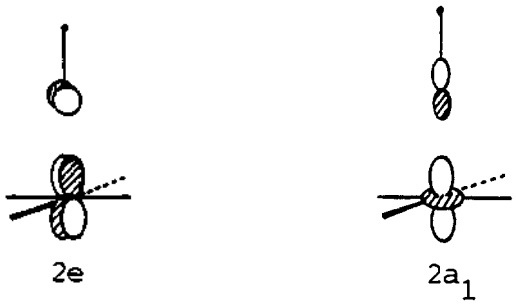

nitude of net destabilization is proportional to the overlap between two orbitals, it is said that the large contributed of the destabilization comes from the molecular orbital, $2a_1$, because the hybridization of $s + z$ of chlorine extends toward z^2 in an antibonding character. Accordingly, the major reason that the total energy abruptly arises can be interpreted as an ineffective interaction of orbital $2a_1$.

Now we turn to the process of breaking one chlorine atom from the intermediate, $Pt(CN)_4Cl_2$. Figure 4 show the potential curve as a function of r, with the distance between platinum and chloride fixed. As a chlorine atom is broken from a coordinated chlorine, the total energy becomes lower, forming a relatively stable intermediated, $Pt(CN)_4Cl$. When the distance between two chlorine is over 3.2 Å, the Figure

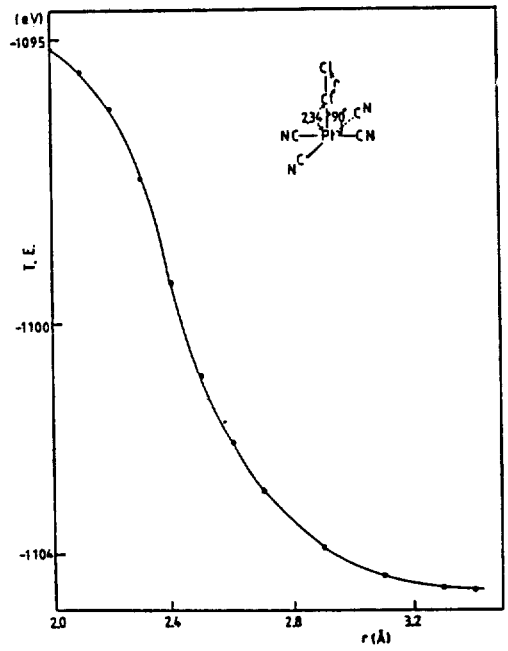

Figure 4. Potential curve as a function of r.

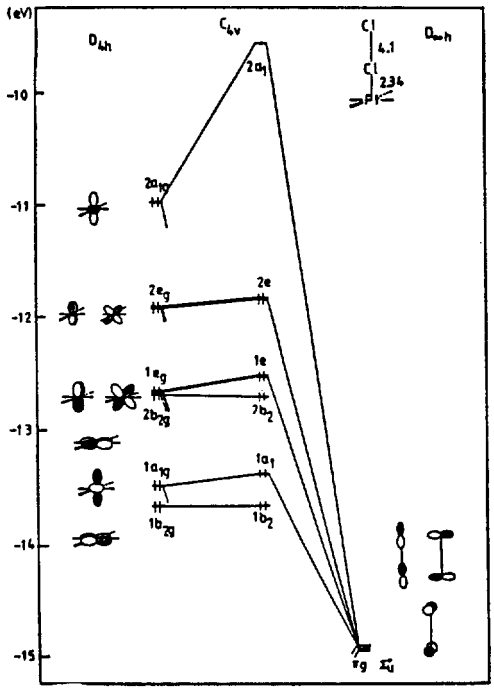

Figure 5. Correlation diagram of orbitals of $Pt(CN)_4Cl_2$ with D_{4h} $Pt(CN)_4$ and $D_{\infty h}$ Cl_2.

shows that there is no substantial interaction between two chlorine atoms. From the Figure, we note that a chlorine atom is spontaneously removed from a coordinated chlorine atom as soon as an unstable intermediate, $Pt(CN)_4Cl_2$, is formed, without loss of energy.

The electronic structure of $(CN)_4PtCl....Cl$ is easily constructed by interacting a $(CN)_4Pt^{1+}$ fragment with a $Cl....Cl^{1-}$ atom. This is done in Figure 5. On the left side of this Figure are the important valence orbitals of the $(CN)_4Pt^{1+}$ fragment. This fragment is supposed to be not distorted from planarity and therefore the valence orbitals are very close to what one

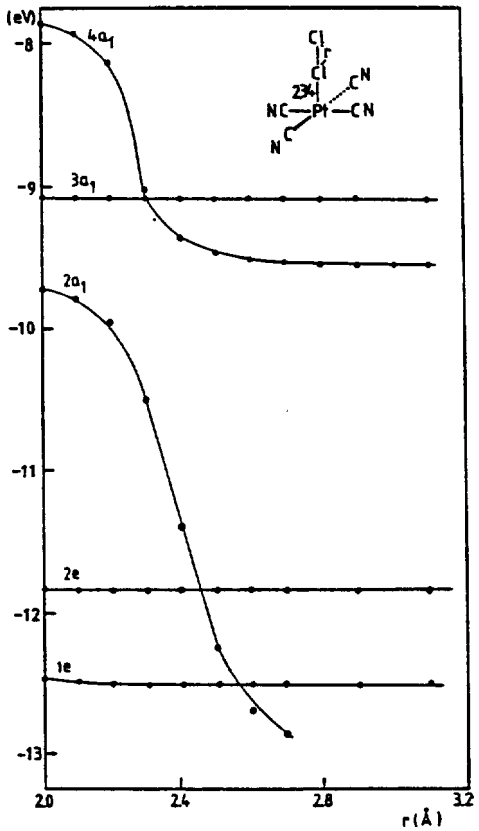

Figure 6. Walsh diagram of a C_{4v} $Pt(CN)_4$ Cl_2 fragment as a function or r.

would expect for a D_{4h} ML_4 complex. At high energy is a primarily metal z^2 orbital of $2a_{1g}$ symmetry followed by an e set of xz and yz character. At low energy is an e set of predominantly metal xz and yz character and xy, which has $2b_{2g}$ symmetry. Normally xy is expected to lie above the xz/yz set when there are σ-donor ligands around the metal. However, strong π bonding from the cyanide lone pairs inverts this orbital sequence. The atomic x and y orbitals on chloride interact with the xz/yz set to produce bonding molecular orbitals (not shown in the Figure) and slightly antibonding counterparts, $1e$ and $2e$. The xy and x^2-y^2 set does not overlap to an appreciable extent with the chloride atomic orbitals because of its δ symmetry. Consequently metal xy and x^2-y^2 orbitals remain nonbonding. Metal z^2 orbital ($1a_{1g}$ and $2a_{1g}$) interacts with the z orbital on chloride to produce bonding molecular orbitals (not shown in the Figure) and antibonding counterparts, $1a_1$ and $2a_1$. The $2e$ level can be identified with the filled lone pair at the platinum atom and is predicted to be the HOMO in the product. It is predominantly chloride x and y in character, mixed in an slightly antibonding way to platinum xy/yz orbitals. The LUMO, $2a_1$, consists of a combination of z^2 orbital on platinum atom and z orbital on chloride atom in an antibonding fashion. The stabilization of a $(CN)_4PtCl....Cl$ intermediate compared with $(CN)_4PtCl$-Cl intermediate will be achieved by a result of electron transfer from z^2 orbital on platinum atom to lower bonding orbital, giving rise to diminishing the level of antibonding orbital.

Figure 6 shows a Walsh diagram as a function of r, with the distance of Pt-Cl fixed. The variation in r produces only slight energy changes within the lower two orbital bonds, but the orbitals derived from $2a_1$ and $4a_1$, respectively, are subs-

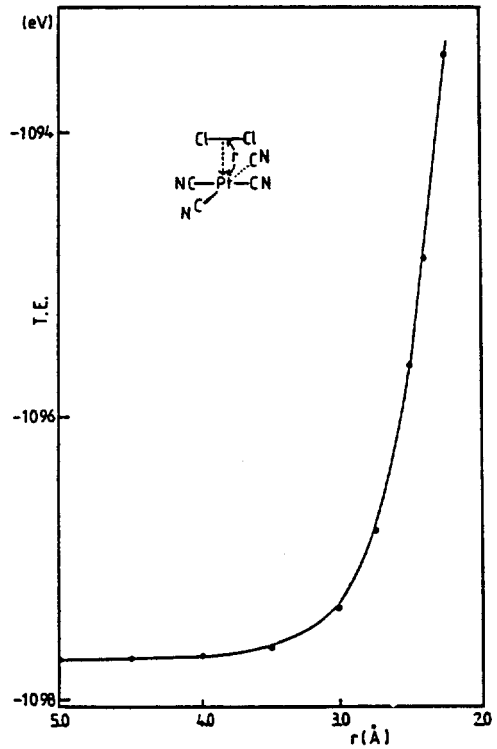

Figure 7. Total energy curve as a function of r.

tantially affected; $2a_1$ and $4a_1$ come down in energy. This behavior of $2a_1$ and $4a_1$ is easily understood by examining the shape of these orbitals as shown in 1.

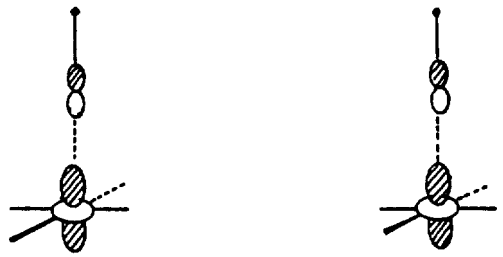

1

As r is increased, the overlap between two chloride atoms will be decreased and this results in the Pt-Cl antibonding orbitals $2a_1$ and $4a_1$ being stabilized. The rapid change of $2a_1$ orbital in energy compared with $4a_1$ orbital can be interpreted by strong interaction of the Pt-Cl antibonding character.

Three Centered Transition State. We now examine the case that occurs in three centered transition state. In introduction section we indicated the significant differences in structure between 1*a* and 1*b*. In order to examine the change of electronic contribution when the attack is changed from 1*a* to 1*b*, we deal with three centered transition state.

In Figure 7 is the total energy curve for variation of the distance r. Like the linear transition state, until the distance is over 4 Å, there is no substantial interaction between two atoms. However, as the distance is getting close, the energy will be abruptly increased. When the distance is approached in bonding distance (2.34 Å), the energy difference in two intermediates between linear transition state and three centered transition state is 6.99 kcal/mol, the linear transition state

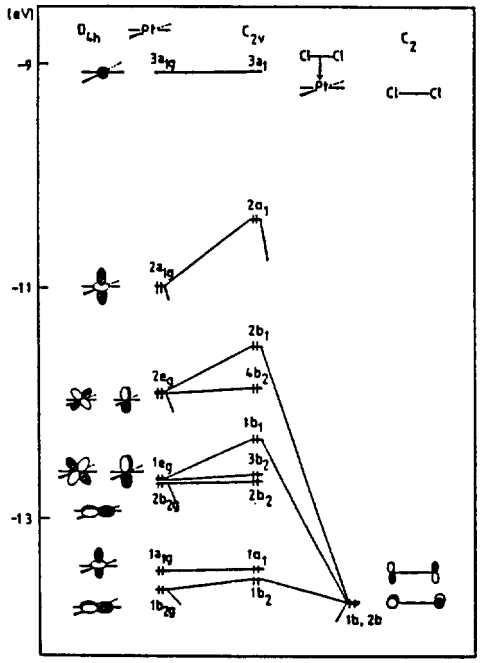

Figure 8. Correlation diagram of orbitals of $Pt(CN)_4Cl_2$ with D_{4h} $Pt(CN)_4$ and C_2Cl_2.

being more stable than three centered transition state.

Figure 8 shows the interaction diagram for a chloride ligand and a $Pt(CN)_4$ fragment. The filled $1b$ and $2b$ orbitals of the Cl_2 fragment interact strongly with the $1e_g$ and $2e_g$ orbitals of the $Pt(CN)_4$ fragment. In addition, the chloride p orbitals mix with the filled $1b_{2g}$ orbital. At higher energy $1a$ interacts with z^2 in a bonding and antibonding fashion to produce Pt<Cl Cl σ and σ^* bonds. The most important of these interactions is between chloride p and $2a_{1g}$ since the antibonding combination resulting from this mixing becomes the HOMO of the intermediate. The HOMO has significant chloride p character (~52%). As indicated before, the unstability of three centered transition state compared with linear transition state arises from two orbitals, $1b_1$ and $2b_1$. As seen from Figure 2, the corresponding $1e$ and $2e$ orbitals are essentially nonbonding. However, in three centered transition state the filled two orbitals, $1b_1$ and $2b_1$, have to an appreciable extent antibonding character. In contrast to that, the HOMO, $2a_1$, in Figure 8 is stabilized in comparison with that in Figure 2. The reason for this difference lies in the ineffective overlap in an antibonding fashion. Accordingly, as the gain of energy in the orbital, $2a_1$, can not be compensated for the loss of energy in two orbitals, $1b_1$ and $2b_1$, the intermediate in three centered transition state will be unstable compared with that in the linear transition state.

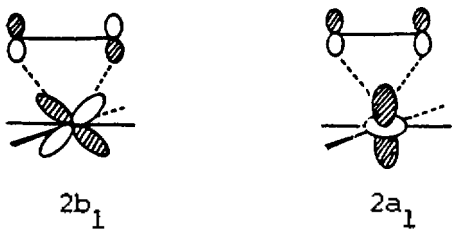

Figure 9 shows a Walsh diagram as a function of r. Among various orbitals, two orbitals derived from $2a_1$ and

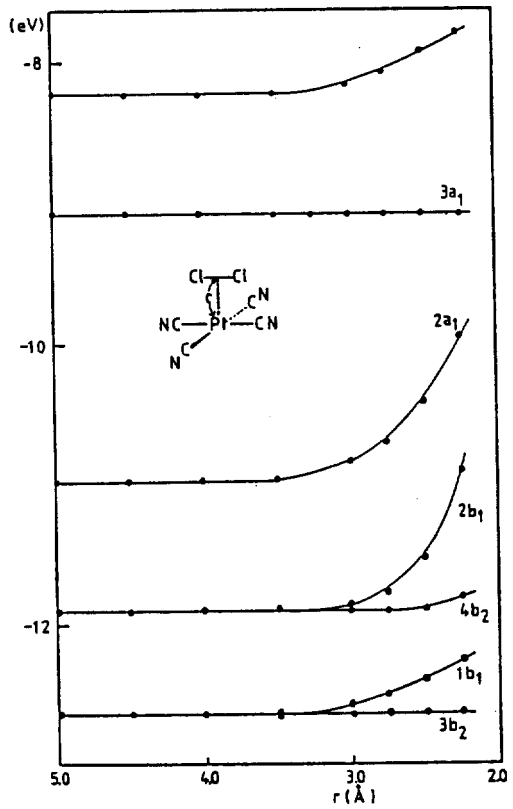

Figure 9. Walsh diagram of a C_{4v} $Pt(CN)_4Cl_2$ fragment as a function of r, with fixed Cl–Cl distance.

$2b_1$ are substantially affected for the variation in r, as described above.

The salient features of this generalized analysis can be summaried as follows:

(1) The transient intermediate proceeding with linear transition state is more favourable than that with three centered transition state.

(2) As a chlorine molecule is approached to a $(TBA)_2$ $Pt(CN)_4$ enough to have a bonding interaction, an uncoordinated chloride atom is forced to point away from a coordinated chloride atom due to an antibonding character, the resulting transition state $(TBA)_2Pt(CN)_4Cl$ becoming more stable.

(3) The free chloride atom immediately adds to the $(TBA)_2$ $Pt(CN)_4Cl$ intermediates in the trans configuration with the energy in gain.

Comparison with Experimental Results

When two ligands are oxidatively added to the $(TBA)_2Pt(CN)_4$, they can enter in one of two orientations, either trans or cis to each other. If the ligands are added to the $(TBA)_2Pt(CN)_4$ in the trans configuration, the symmetry about Pt would be D_{4h} and one CN stretching mode (E_u) would be expected in the ν (CN) region of the infrared spectrum. On the other hand, if the ligands are added in the cis configuration, the symmetry about Pt would be C_{2v} and four CN stretching modes ($2A_1 + B_1 + B_2$) would be expected in the infrared spectrum. From the data, which shows that there is one stretching mode of CN, it is clear that the added ligands are trans to each other. A similar example was appeared in other instants. This result is in good agreement with that of extended Hückel calculations.

Table 1. Extended Huckel Calculation Parameters

Atom	Orbital	H_{ii}(eV)	ξ_{i1}	$(C_1)^a$	ξ_{i2}	$(C_2)^a$	ref.
Pt	6*s*	-9.077	2.554				*b*
	6*p*	-5.475	2.554				
	5*d*	-12.59	6.013	(0.6334)	2.696	(0.5513)	
Cl	3*s*	-26.3	2.183				*c*
	3*p*	-14.2	1.733				
C	2*s*	-21.4	1.625				*c*
	2*p*	-11.4	1.625				
N	2*s*	-26.00	1.95				*c*
	2*p*	-18.60	1.95				

[a] C_1 and C_2 are coefficients in a double ξ expansion. [b] H. Basch and H. B. Gray, *Theor. Chim. Acta.*, **4**, 367 (1966). [c] R. H. Sumerville and R. Hoffmann, *J. Am. Chem. Soc.*, **98**, 7240 (1976).

Appendix

The Pt–C and C–N distances are based on the paper.[8] The extended Hückel calculations used a modified Wolfsberg–Helmholz formula with the parameters listed in Table 1. Orbital exponents and H_{ii}'s for Pt was obtained from previous work.[b]

Acknowledgement. This work was supported by a Grant-in-Aid for Free Research Project from the Ministry of Education, Korea.

References

1. (a) J. Halpern, T. Okamoto, and A. Zakhariev, *J. Mol. Cat.*, **2**, 65 (1976); (b) C. K. Brown and G. Wilkinson, *J. Chem. Soc. (A)*, 2753 (1970); (c) R. L. Pruett and J. A. Smith, *J. Org. Chem.*, **34**, 327 (1969).
2. (a) J. P. Collman and W. R. Roper, *Adv. Organomet. Chem.*, **7**, 53 (1968); (b) R. Ugo, *Coord, Chem. Rev.*, **3**, 319 (1968).
3. (a) J. D. Ruddick and B. L. Shaw, *J. Chem. Soc. (A)*, 2964 (1969); (b) J. D. Ruddick and B. L. Shaw, *J. Chem. Soc. (A)*, 2801 (1969); (c) R. J. Puddephatt and C. E. E. Upton, *J. Organomet. Chem.*, **91**, C17 (1975); (d) M. P. Brown, R. J. Puddephatt, and C. E. E. Upton, *J. Chem. Soc., Dalton. Trans.*, 2457 (1974); (e) A. J. Cheney and B. L. Shaw, *J. Chem. Soc. (A)*, 3545 (1971); (f) A. J. Cheney and B. L. Shaw, *J. Chem. Soc. (A)*, 3549 (1971); (g) C. R. Kistner, J. H. Hutchinson, J. R. Doyle, and J. C. Storlie, *Inorg. Chem.*, **2**, 1255 (1963).
4. R. Osso and J. V. Rund *J. Coord. Chem.*, **8**, 169 (1978).
5. (a) J. P. Collmann, *Acc. Chem. Res.*, **1**, 136 (1968); (b) J. Halpern, *Acc. Chem. Res.*, **3**, 486 (1968); (c) L. Vaska, *Acc. Chem. Res.*, **1**, 335 (1968).
6. R. Hoffmann and W. N. Lipscomb, *J. Chem. Phys.*, **36**, 2179 (1962).
7. J. A. Abys, G. Ogar, and W. M. Risen, Jr., *Inorg. Chem.*, **20**, 4446 (1981).
8. (a) J. S. Miller, "Extended Linear Chain Compounds", Vol. I, Plenum, New York (1982); (b) M. H. Whangbo and M. J. Foshee, *Inorg. Chem.*, **20**, 113 (1981).